Low bending loss characteristics of hybrid plasmonic waveguide for flexible optical interconnect

Jin Tae Kim,[1,3] Suntak Park,[1] Jung Jin Ju,[1] Sangjun Lee,[2] and Sangin Kim[2,4]

[1]*Convergence Components and Materials Research Laboratory, ETRI, Daejeon 305-700, Korea*
[2]*Department of Electrical and Computer Engineering, Ajou University, Suwon 443-749, Korea*
[3]*jintae@etri.re.kr*
[4]*sangin@ajou.ac.kr*

Abstract: The bending loss characteristics of the hybrid plasmonic waveguide are investigated theoretically and experimentally. Simulation results showed that the guided mode is confined mainly into outer high index slab as the bending radius decreases. Thus, the radiation loss due to bending is greatly suppressed. We fabricate flexible hybrid plasmonic waveguide consisted of 5 nm-thick Au stripe and flexible multiple polymer cladding layers. The measured bending loss is lower than 1 dB/180° at a wavelength of 1310 nm for the bending radii down to 2 mm.

OCIS codes: (240.6680) Surface plasmons; (230.7370) Waveguides; (130.3120) Integrated optics devices.

References and links

1. A. D. Boardman, ed., *Electromagnetic Surface Modes* (Wiley, 1982).
2. W. L. Barnes, A. Dereux, and T. W. Ebbesen, "Surface plasmon subwavelength optics," Nature **424**(6950), 824–830 (2003).
3. D. Sarid, "Long-range surface-plasma waves on very thin metal films," Phys. Rev. Lett. **47**(26), 1927–1930 (1981).
4. P. Berini, "Plasmon-polariton waves guided by thin lossy metal films of finite width: Bound modes of symmetric structures," Phys. Rev. B **61**(15), 10484–10503 (2000).
5. T. Nikolajsen, K. Leosson, and S. I. Bozhevolnyi, "Surface plasmon polariton based modulators and switches operating at telecom wavelengths," Appl. Phys. Lett. **85**(24), 5833–5835 (2004).
6. R. Charbonneau, N. Lahoud, G. Mattiussi, and P. Berini, "Demonstration of integrated optics elements based on long-ranging surface plasmon polaritons," Opt. Express **13**(3), 977–984 (2005).
7. S. Jetté-Charbonneau, R. Charbonneau, N. Lahoud, G. Mattiussi, and P. Berini, "Demonstration of Bragg gratings based on long-ranging surface plasmon polariton waveguides," Opt. Express **13**(12), 4674–4682 (2005).
8. A. Boltasseva, T. Nikolajsen, K. Leosson, K. Kjaer, M. S. Larsen, and S. I. Bozhevolnyi, "Integrated Optical Components Utilizing Long-Range Surface Plasmon Polaritons," J. Lightwave Technol. **23**(1), 413–422 (2005).
9. S. Jetté-Charbonneau, and P. Berini, "External cavity laser using a long-range surface plasmon grating as a distributed Bragg reflector," Appl. Phys. Lett. **91**(18), 181114 (2007).
10. S.-Y. Park, J. T. Kim, J.-S. Shin, and S.-Y. Shin, "Hybrid vertical directional coupling between a long range surface plasmon polariton waveguide and a dielectric waveguide," Opt. Commun. **282**(23), 4513–4517 (2009).
11. J. T. Kim, J. J. Ju, S. Park, M. S. Kim, S. K. Park, and M.-H. Lee, "Chip-to-chip optical interconnect using gold long-range surface plasmon polariton waveguides," Opt. Express **16**(17), 13133–13138 (2008).
12. J. T. Kim, J. J. Ju, S. Park, S. K. Park, M. Kim, J.-M. Lee, J.-S. Choe, M.-H. Lee, and S.-Y. Shin, "Silver stripe optical waveguide for chip-to-chip optical interconnection," IEEE Photon. Technol. Lett. **21**(13), 902–904 (2009).
13. W.-K. Kim, W.-S. Yang, H.-M. Lee, H.-Y. Lee, M. H. Lee, and W. J. Jung, "Leaky modes of curved long-range surface plasmon-polariton waveguide," Opt. Express **14**(26), 13043–13049 (2006).
14. P. Berini, and J. Lu, "Curved long-range surface plasmon-polariton waveguides," Opt. Express **14**(6), 2365–2371 (2006).
15. S. Lee, S. Kim, and H. Lim, "Improved bending loss characteristics of asymmetric surface plasmonic waveguides for flexible optical wiring," Opt. Express **17**(22), 19435–19443 (2009).
16. J.-M. Lee, S. Park, M. S. Kim, S. K. Park, J. T. Kim, J.-S. Choe, W.-J. Lee, M.-H. Lee, and J. J. Ju, "Low bending loss metal waveguide embedded in a free-standing multilayered polymer film," Opt. Express **17**(1), 228–234 (2009).
17. J. T. Kim, J. J. Ju, S. Park, M. S. Kim, S. K. Park, and S.-Y. Shin, "Hybrid plasmonic waveguide for low-loss lightwave guiding," Opt. Express **18**(3), 2808–2813 (2010).
18. E. D. Palik, *Handbook of Optical Constants of Solids* (Academic, 1985).

#133618 - $15.00 USD Received 18 Aug 2010; revised 7 Oct 2010; accepted 18 Oct 2010; published 4 Nov 2010

19. G. L. Xu, W. P. Huang, M. S. Stern, and S. K. Chaudhuri, "Full-vectorial mode calculations by finite difference method," IEE Proc., Optoelectron. **141**(5), 281–286 (1994).
20. R. Mittra, and U. Pekel, "A new look at the perfectly matched layer (PML) concept for the reflectionless absorption of electromagnetic waves," IEEE Microw. Guid. Wave Lett. **5**(3), 84–86 (1995).
21. J. T. Kim, S. Park, J. J. Ju, S. K. Park, M.-S. Kim, and M. H. Lee, "Low-loss polymer-based long-range surface plasmon-polariton waveguide," IEEE Photon. Technol. Lett. **19**(18), 1374–1376 (2007).
22. J. T. Kim, S. Park, and S. K. Park, "M.- Kim, M.-H. Lee, and J. J. Ju, "Gold stripe optical waveguides fabricated by a novel double-layered liftoff process," ETRI J. **31**(6), 778–783 (2009).
23. I.-S. Jeong, H.-R. Park, S.-W. Lee, and M.-H. Lee, "Polymeric waveguides with Bragg gratings in the middle of the core layer," J. Opt. Soc. Korea **13**(2), 294–298 (2009).
24. P. Gadenne, and G. Vuye, "In situ determination of the optical and electrical properties of thin films during their deposition," J. Phys. E **10**(7), 733–736 (1977).

1. Introduction

A transverse magnetic (TM) polarized electromagnetic surface wave is allowed at the interface between a metal and a dielectric medium [1]. This surface wave is called surface plasmon polariton (SPP) because it is associated with the coupling between collective oscillation of free electrons in the metal and electromagnetic waves. Since the SPP can be confined within very small area beyond the diffraction limit, SPP-based waveguides hold huge potential for the development of novel integrated optical devices in subwavelength scale [2].

Besides the applications in nano-photonic devices, the SPPs are also useful for long-range propagation-based applications such as optical interconnect if their propagation lengths are properly engineered. In a thin metal film, the SPPs excited at two metal-dielectric interfaces are couple each other and two types of super modes of different symmetries are formed: One is a short-range SPP(SRSPP) mode of odd symmetry and the other a long-range SPP (LRSPP) mode of even symmetry [3]. The LRSPP mode shows an enhanced propagation distance of cm scale at optical communication wavelength. Based on the LRSPP, a thin metal stripe optical waveguide has been proposed [4], and numerous optical devices using the metal stripe waveguides have been demonstrated [5–10]. Especially, the metal stripe waveguides embedded in polymer cladding layers appear attractive and versatile in device applications because the polymer materials provide easy fabrication process, low absorption loss and high thermo-optic coefficient. Recently, optical interconnections using metal stripes embedded in uniform low loss polymer claddings have been demonstrated. 2.5 Gbps chip-to-chip optical interconnect was demonstrated at a wavelength of 1310 nm using a gold-stripe waveguide [11]. 2.5 Gbps optical signal transmission over 10 cm-long silver-stripe LRSPP waveguide was also successfully demonstrated [12].

Chip-to-chip optical interconnection using metal stripe optical waveguides could be deployed as an optical bus for board-to-board optical communication. One potential application is the interconnection between the main body and the display section in hand-held devices such as labtop computers and cellular phones. In practical board-to-board optical interconnect applications, flexible optical waveguides are highly required. Since the polymer materials used in this research are very flexible, the LRSPP waveguide based on the metal stripe embedded in the polymer materials may be a possible candidate for the flexible optical interconnect. However, theoretical studies have revealed that the metal stripe waveguides with uniform claddings show poor bending loss characteristics which are not suitable for practical applications [13,14]. So, there have been efforts to improve the bending loss characteristics of the metal stripe waveguide by adopting non-uniform cladding structures [15,16]. Metal stripe optical waveguides with asymmetric cladding layers has been suggested and their performance improvement has been theoretically investigated [15]. A metal stripe embedded in multilayered polymer film was proposed for a low banding loss, where a central polymer layer of higher refractive index provides additional index-guiding and results in low bending loss [16]. The fabricated waveguide showed very low vertical bending loss of 0.3 dB/ 180 ° for bending radii down to 2 mm. In this structure, however, the additional index-guiding effect in the high index cladding layer causes a drawback of propagation loss increase in a straight waveguide compared to the uniform cladding structure due to the increased field confinement in the metal stripe core embedded in the high index core layer.

#133618 - $15.00 USD Received 18 Aug 2010; revised 7 Oct 2010; accepted 18 Oct 2010; published 4 Nov 2010

Recently, we proposed and experimentally demonstrated a new type of a hybrid plasmonic waveguide structure in which a metal stripe was embedded in a low index polymer layer surrounded by two high index slabs [17]. In the proposed structure, field confinement in the metal stripe is reduced and thus, the propagation loss is greatly lowered compared to the structure with a uniform cladding. In general, the metal stripe waveguide with a uniform cladding shows trade-off between propagation and bending losses, that is, the propagation loss increase is inevitable to lower the bending loss. Whereas, the proposed hybrid plasmonic waveguide is expected to show a low bending loss in spite of the reduced field confinement in the metal stripe because the surrounding high index slabs may suppress a radiation due to bending. In this paper, we report the numerical and experimental investigations on the bending loss characteristics of the hybrid plasmonic waveguide. Numerical simulation confirms the role of the surrounding high index slabs to suppress a bending loss. The bending losses of a fabricated hybrid plasmonic waveguide have been measured for various bending radii.

2. Architectural concepts and theoretical analysis

Figure 1 shows the bent waveguide structure of the previously proposed hybrid plasmonic waveguide [17]. As seen in Fig. 1(b), the waveguide consists of a gold stripe embedded in between two high refractive index slabs. In the mode analysis of the bent waveguide, the same cross sectional geometry and materials as those optimized for the straight waveguide in the previous work are assumed [17]. The refractive indices of the claddings are $n_1 = n_3 = 1.514$, and the refractive index of the slab core is $n_2 = 1.524$. The thicknesses of the inner-cladding and the slab core are $h = 2$ μm and $d = 5$ μm, respectively. The thickness and the width of the gold stripe is $t = 5$ nm and $w = 3.5$ μm, respectively. For comparison, a 5 μm-wide gold stripe is also considered in the calculation. The complex refractive index of Au is assumed to be 0.4081–8.305*i* at a wavelength of 1310 nm [18].

To analyze the guided mode of the bent waveguides, the full-vector finite difference method (FDM) in a cylindrical coordinate is used [15,19] with the perfectly matched layer absorbing boundary condition adopting the stretched coordinate concept [20]. In the FDM, Helmholtz's equations are discretized with a rectangular grid over the cross-section of the waveguide and solved numerically. In our calculations, a non-uniform grid is used to save computer memory; the inside of and the region near the metal stripe, the grid size of 1 nm is used, and in other region, the grid size is λ/20 ~λ/10.

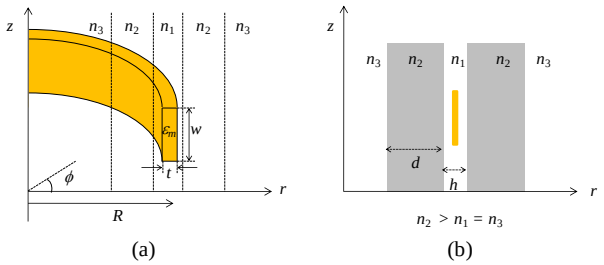

Fig. 1. Architectural view of curved hybrid plasmonic waveguide bend. (a) perspective view and (b) cross-sectional view.

Figure 2 shows the calculated dominant field (E_r) contour plots and profiles of the curved hybrid plasmonic waveguides of various bending radii with $w = 3.5$ μm. Without the metal stripe, the waveguide structure is considered as a dual core slab waveguide with high refractive-index contrast. If the distance h is small enough for light to couple from one core waveguide to the other, the whole structure of core layers must be analyzed to get the symmetric super-modes. The symmetric slab mode is confined in the lateral direction. However, the mode is not confined in the vertical direction because of infinite core height. The vertical confinement of mode is possible by embedding a metal stripe in the inner-cladding layer, as shown in Fig, 2 (a). The symmetric hybrid mode is like a combination of the symmetric LRSPP strip mode and a dual symmetric dielectric slab mode [17].

#133618 - $15.00 USD Received 18 Aug 2010; revised 7 Oct 2010; accepted 18 Oct 2010; published 4 Nov 2010

For a large bending radius, i.e. R = 100 mm, the field profile is similar to that of the straight waveguide whose guided mode is like a combination of a LRSPP strip mode (ss_b^0 mode) and a dual symmetric dielectric slab mode [17]. The field is confined mainly in two slabs, which is a key feature of the proposed waveguide lowering the propagation loss, and the outer (in the radial direction) slab confines slightly more field due to bending effect. As the bending radius decreases, the E_r field amplitude of the outer slab increases gradually and the mode becomes highly asymmetric in r direction. For a very small bending radius (R = 5 mm), the field is confined mainly in the outer slab, but the confinement in r direction is still tight and strong. This strong confinement by the high index slab will suppress radiation loss of bending and provide a low bending loss down to a very small bending radius. Another thing to note is that the field amplitude at the metal surface decreases as the bending radius decreases, which will also result in a lower bending loss for a small bending radius.

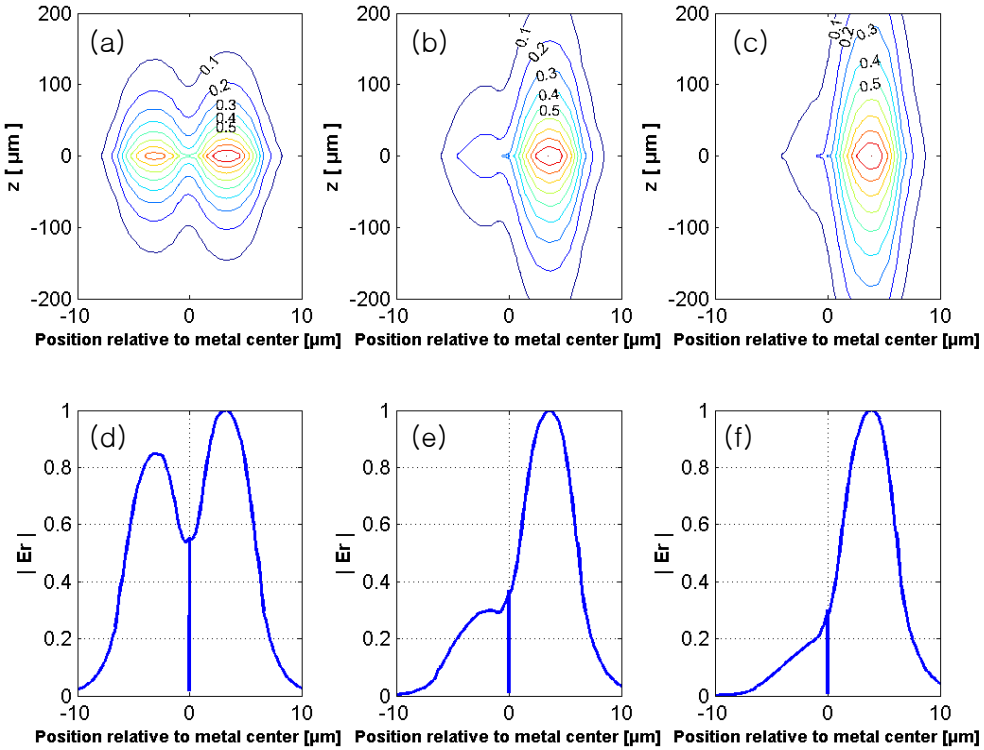

Fig. 2. E_r field contour plots and E_r field distributions along z = 0 line in the curved hybrid plasmonic waveguides of various radii: (a) & (d) R = 100 mm, (b) & (e) R = 10 mm, and (c) & (f) R = 5 mm. h = 2 μm, d = 5 μm, w = 3.5 μm, t = 5 nm in all cases.

Figure 3 shows the calculated propagation characteristics of the curved hybrid plasmonic waveguides of various bending radius. For comparison, two metal stripes with different widths, 3.5 and 5.0 μm, are considered. The effective refractive index increases as the curvature radius decreases, as shown in Fig. 3(a). The effective refractive index converges to the value of the corresponding straight waveguide as the bending radius becomes infinite ($r \rightarrow \infty$). Figure 3(b) shows the bending loss of the curved waveguide as a function of the bending radius R. The calculated propagation loss of the straight waveguide of w = 3.5 μm is also plotted as a reference (red line). The bending loss is calculated from the complex propagation constant along Φ direction and the loss per unit radian (dB/radian) is converted to the loss per unit length (dB/mm). So, the calculated bending loss includes both the propagation loss due to metallic loss and the radiation loss due to bending.

The bending loss characteristics of the hybrid plasmonic waveguide exhibits a different tendency from the metal stripe with a uniform cladding whose bending loss increases

#133618 - $15.00 USD Received 18 Aug 2010; revised 7 Oct 2010; accepted 18 Oct 2010; published 4 Nov 2010

continuously with the decrease of the bending radius [13,14]. As seen in Fig. 3(b), the bending loss of the hybrid plasmonic waveguide decreases as R decreases for small R (< ~10 mm). This is attributed to the decreasing field confinement in the metal stripe as R decreases. (See Fig. 2) Moreover, this implies that in the proposed waveguide the radiation loss due to bending does not increase severely even for a very small R because of the strong field confinement of the high index slab. Since the wider metal stripe undergoes the larger metal loss, 5.0 μm-wide metal stripe shows larger bending loss than 3.5 μm-wide one.

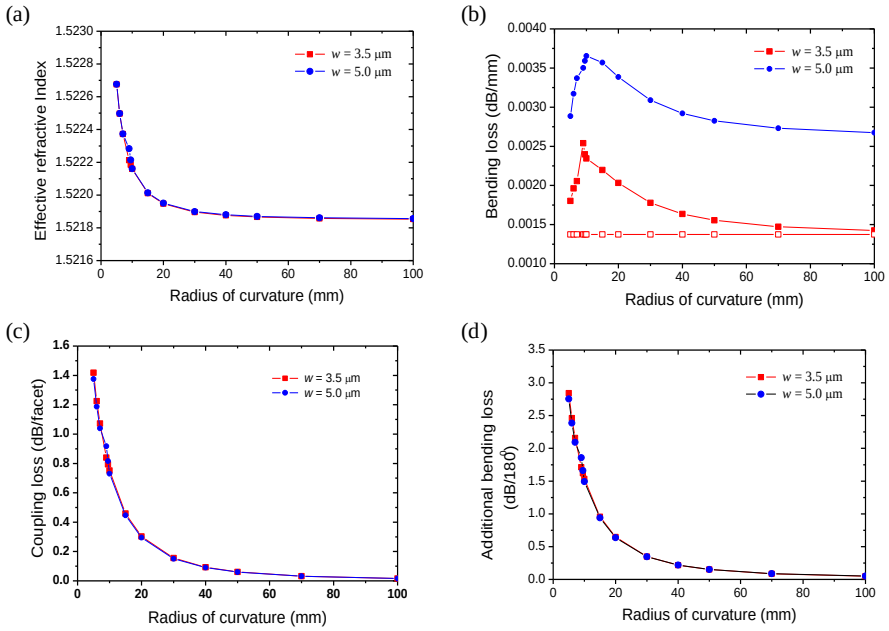

Fig. 3. Calculated propagation characteristics of the curved hybrid plasmonic waveguide. (a) Effective refractive index, (b) bending loss per unit length, (c) coupling loss between the straight and the curved waveguides, and (d) total additional bending loss per 180° as functions of a bending radius. h = 2 μm, d = 5 μm, t = 5 nm in all cases.

The coupling losses between the curved and the straight waveguides are calculated from overlap integrals of their mode profiles and plotted as a function of R in Fig. 3(c). As R decreases, the mode mismatch between the guided modes of the straight and the curved waveguides increases, and thus, the coupling loss increases. Figure 3 (d) shows the calculated total additional bending loss of the hybrid plasmonic waveguide for a 180° bending as a function of R. In the calculation of the additional bending loss, both the bending loss caused by 180° bending and the coupling loss are considered, and the propagation loss of the straight waveguide of the same length as the 180° bending of R is subtracted. In the proposed waveguide, the bending loss of the curved waveguide is well suppressed and thus, the total additional bending loss is attributed mainly to the coupling loss. For instance, the total coupling loss for a bending of R = 5mm is about 2.8 dB considering two facets, and the additional bending loss occurring in the curved waveguide is about 0.004 dB.

The bending loss characteristics of the proposed hybrid plasmonic waveguide is compared to those of the plasmonic waveguide with high-index central layer reported in [16] whose cross-sectional structure is depicted in Fig. 4(a). For fair comparison, the same polymer materials (n_1 = 1.514 and n_2 = 1.524) and the gold stripe of the same dimensions as the proposed waveguide (w = 3.5 μm and t = 5 nm) are used. The thickness of the central polymer layer is 10 μm, which corresponds to the case of h = 0 in the proposed waveguide depicted in Fig. 1(b).

Figure 4(e), 4(f), and 4(g) show the calculated mode profiles of the waveguide reported in [16] for R = 100 mm, 5 mm, and 2 mm, respectively. One can see that the field is more

#133618 - $15.00 USD Received 18 Aug 2010; revised 7 Oct 2010; accepted 18 Oct 2010; published 4 Nov 2010

confined near the metal stripe compared to the proposed waveguide. The calculated bending loss per unit length and the additional bending loss for a 180° bending are plotted as functions of bending radius in Fig. 4(b) and 4(c), respectively. Since the waveguide with high-index central layer has higher field confinement in the metal stripe, it shows less additional bending loss, but its propagation loss is about one order of magnitude larger than the proposed waveguide. Therefore, as seen in Fig. 4(d), the total loss (including the propagation loss) of a 180° bending of the waveguide with high-index central layer increases rapidly as R increases for $R > 5$ mm. From this comparison, the proposed waveguide appears to be a better choice for optical interconnect applications in that it shows improved bending loss characteristics of a permissible level in practical applications in spite of the greatly reduced propagation loss.

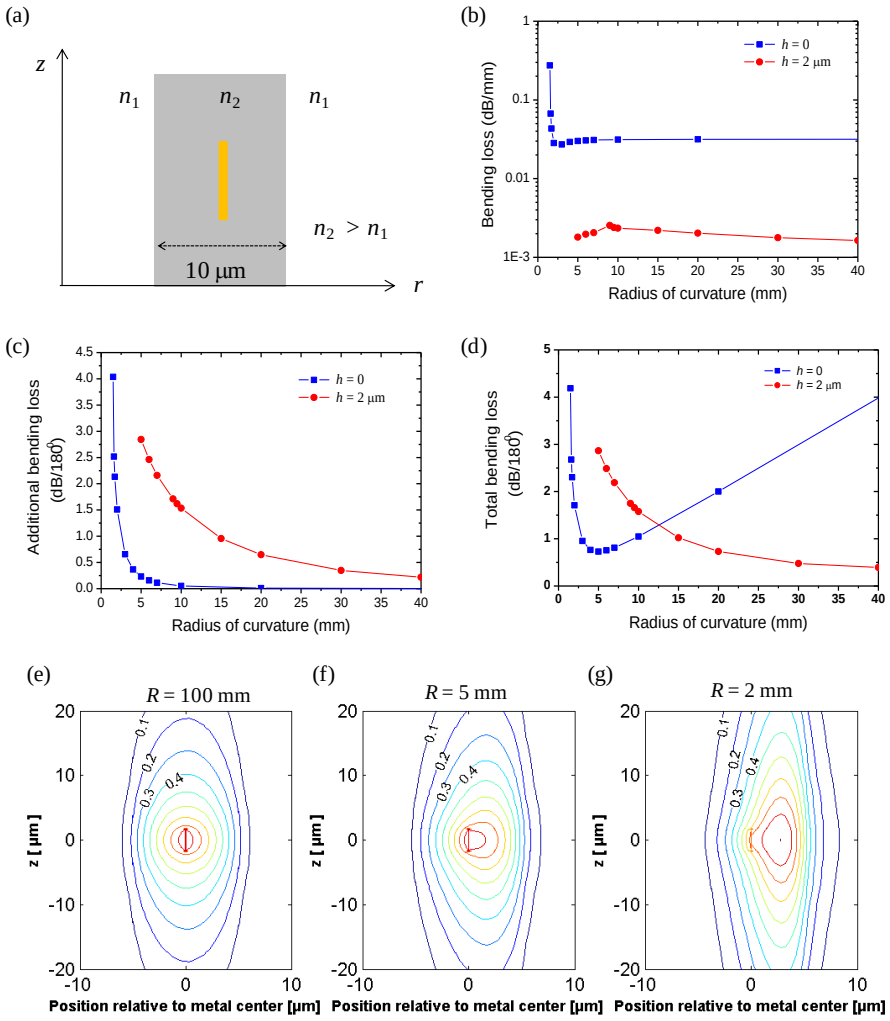

Fig. 4. Comparison between the proposed hybrid plasmonic waveguide (h = 2 μm) and the waveguide reported in [16] (h = 0). (a) Waveguide structure reported in [16], where n_1 = 1.514 and n_2 = 1.524, (b) bending loss per unit length, (c) total additional bending loss per 180° as functions of a bending radius, and (d) total loss of a 180° bending including propagation loss. Mode profiles of the waveguide depicted in (a) for (e) R = 100 mm, (f) R = 5 mm, and (g) R = 2 mm. The dimensions of the metal stripe is the same; w = 3.5 μm, t = 5 nm.

#133618 - $15.00 USD Received 18 Aug 2010; revised 7 Oct 2010; accepted 18 Oct 2010; published 4 Nov 2010

3. Experimental results and discussions

In order to confirm the theoretical investigation, we fabricated the flexible hybrid plasmonic waveguide. For fabrication of dielectric multilayers, a commercial UV-curable polymer, FOWG (ChemOptics) was used. The refractive indices of the cladding and core layer are 1.514 and 1.524, respectively. The detailed fabrication process of the flexible free-standing hybrid plasmonic waveguide is described in the previous reports [16,17,21–23]. For an effective and selective detachment of the waveguide from the Si substrate, 30 nm-thick gold layer is firstly deposited on the central area of the Si substrate. Then, the under-cladding layer was formed to be 20 μm by spin-coating and UV curing. Consequently, the core layer is 5 μm and the inner-cladding is 1 μm. Then, 5 nm-thick Au stripe with 3.5 μm width was evaporated thermally on the pre-patterned AZ 5206E photo-resist. The inner-cladding, core layer, and outer-cladding formed on Au stripes were 1, 5, and 20 μm, respectively. Since the adhesion of the gold layer to the Si substrate is very poor, the central section of the multilayered polymer films is partially detachable from the substrate after the input and output fiber is pigtailed at the ends of the waveguide. The same mechanical component and method as described in the previous report was used to measure the bending loss [16]. For comparison, the bending loss of the standard single mode fiber is measured.

Figure 5 shows the measured additional bending loss of the flexible hybrid plasmonic waveguide and a standard single mode fiber (SMF). The insets depict the fabricated flexible Au hybrid plasmonic waveguide and SMF that are inserted within a bending slot to measure the insertion loss. A 7 cm-long fabricated waveguide was pigtailed to a polarization-maintaining fiber (PMF) at the input side and a SMF at the output side. The fabricated free-standing waveguide was flexible enough to be mechanically bent down to a radius of 0.5 mm. The fiber-to-fiber insertion loss of the straight 7 cm-long hybrid plasmonic waveguide was about 16 dB. The insertion loss of the waveguide did not change significantly after the waveguide is detached from the substrate. Down to R = 15 mm bending, the measured insertion loss did not increase significantly. For R < 10 mm, the insertion loss increased gradually and the additional bending loss for 180° bending of R = 2 mm was measured to be about 1 dB at a wavelength of 1310 nm. The measured value is lower than that of a SMF, whose additional bending loss for 180° bending of R = 6 mm was measured to be 2.3 dB at a wavelength of 1310 nm. Down to R = 4 mm bending, the additional bending loss of a SMF significantly increases up to 15 dB for 180° bending.

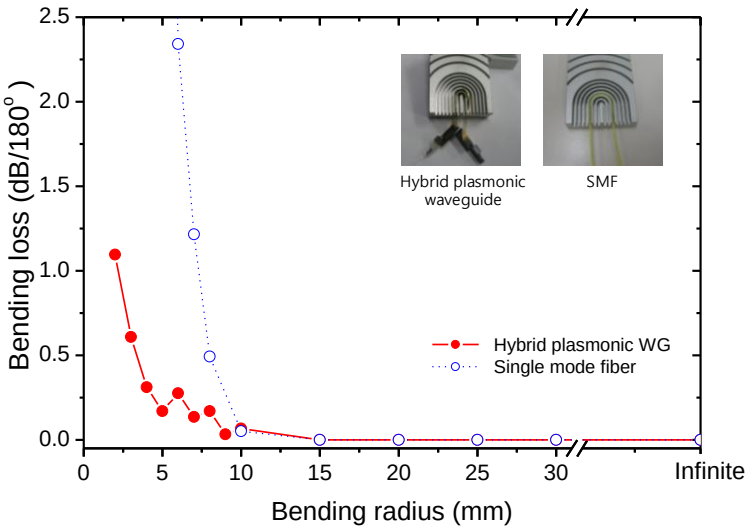

Fig. 5. Measured additional bending and insertion loss of the flexible hybrid plasmonic waveguide and a standard single mode fiber.

#133618 - $15.00 USD Received 18 Aug 2010; revised 7 Oct 2010; accepted 18 Oct 2010; published 4 Nov 2010

The measured additional bending loss is lower than the theoretical prediction. This is partially attributed to the inaccurate refractive index of Au. The refractive index used in the calculation is measured for bulk Au. When the evaporated metal film is extremely thin, the density of the metal film decreases and it may result in the permittivity change of the metal [24]. More importantly, in the coupling loss calculation, an abrupt junction between the straight and the curved waveguides was assumed, but in the measurement setup depicted in the inset in Fig. 4, the junction was gradual since the slots in the holder was much wider than the waveguide. Therefore, the adiabatic mode change between the straight and the curved waveguides might occur and thus, the coupling loss due to the mode mismatch might be relieved.

For practical board-to-board optical interconnect application in commercial hand-held devices, low insertion loss of the optical waveguide is highly required. We have to optimize the trade-off between propagation loss and coupling loss when the hybrid plasmonic waveguide is used for optical interconnects. Unsatisfactory coupling loss may be improved by placing the wide metal stripe with low coupling loss at the input and output ends [17]. On the other hand, the flexible hybrid plasmonic waveguide is easily fabricated by simple three steps: formation of multiple under-cladding using spin-coating and UV-curing, configuring thin metal stripes, and formation of multiple upper-cladding. Deep dry etching or imprinting process that increases the cost for fabricating the thick rectangular core is not required. In addition, it has good mechanical stability in repeated bending due to the thin film nature of the metals. Therefore, hybrid plasmonic waveguide has been considered an alternative candidate to replace the conventional optical guiding mediums in short-range inter-board optical interconnection technology.

4. Conclusion

The bending loss characteristics of the recently proposed hybrid plasmonic waveguide have been investigated theoretically and experimentally. The guided mode analysis in the curved waveguide has revealed that the radiation loss due to bending is greatly suppressed by the strong field confinement of the outer high index slab in the proposed waveguide, and field redistribution in the curved waveguide even reduces bending loss for a very small bending radius. According to the theoretical investigation, the dominant loss component in the bending of the proposed waveguide seems to be the coupling loss due to the mode mismatch between the straight and the curved waveguides. Since an abrupt junction is not likely occurred in practical optical interconnect applications, the coupling loss is expected to be smaller than the theoretical prediction for the abrupt junction. The proposed hybrid plasmonic waveguide has been fabricated and its bending loss has been measured. The measured additional bending losses were lower than 1 dB/180° for the bending radii down to 2 mm. It seems that the lower measured bending loss results from a relieved coupling loss due to a gradual junction between the straight and the curved waveguide in the experimental setup.

Acknowledgements

The first author, J. T. Kim, is grateful to Professor Sang-Yung Shin of KAIST for the insightful comments. This work was supported by the IT R&D program of the MKE/KEIT, Korea (2006-S-073-04) and the S/W Computing R&D program of MKE/KEIT, Korea (10035360-2010-01, TAXEL: Visio-haptic Display and Rendering Engine). This work was also partly supported by National Research Foundation of Korea Grants (NRF-2010-0000217, NRF-2010-0001859).

#133618 - $15.00 USD Received 18 Aug 2010; revised 7 Oct 2010; accepted 18 Oct 2010; published 4 Nov 2010